2016 IEEE International Conference on Technological Innovations in ICT For Agriculture and Rural Development (TIAR 2016)

Precision farming using Unmanned Aerial and Ground Vehicles

Ashwin Vasudevan
EIE Department
Easwari Engineering College
contact@ashwinvasudevan.com

Ajith Kumar. D
EIE Department
Easwari Engineering College
ajithofficials@gmail.com

Dr. N. S. Bhuvaneswari
HOD, EIE Department
Easwari Engineering College
hod.eie@srmeaswari.ac.in

***Abstract*—The primary goal of this project is to design and implement a fully autonomous UAV (Unmanned Aerial Vehicle) for precision agriculture and farm management. It provides high resolution, spectral images in narrowband blue, green, red, red edge, and near-infrared bands. The secondary goal of this project is to develop a UGV (Unmanned Ground Vehicle) equipped with multiple sensors to provide a high level of autonomy for environmental modeling and to obtain real time images. Images from the UAV and the UGV are then processed with specific indices such as Normalized Difference Vegetation Index [NDVI], Renormalized Difference Vegetation Index [RDVI], Optimized Soil Adjusted Vegetation Index [OSAVI], D. Enhanced Normalized Difference Vegetation Index [ENDVI], Soil Adjusted Vegetation Index [SAVI] to obtain useful output for farm management.**

***Index Terms*—Unmanned aerial vehicles, Terrain mapping , Simultaneous localization and mapping, Vegetation.**

I. INTRODUCTION

It is estimated that we need about 70% more food in 2050 than we have today in order to provide every one of the 9.6 billion world population with a daily intake of 3,000 calories. Addressing the challenges of feeding the burgeoning world population with limited resources requires innovation in sustainable, efficient farming. The practice of precision agriculture offers many benefits towards addressing these challenges, such as improved yield and efficient use of such resources as water, fertilizer and pesticides. An unmanned aerial vehicle (UAV) and an unmanned ground vehicle (UGV) was assembled and tested with the aim of developing a flexible and powerful tool for site-specific farming management. The basic idea is to make the Unmanned aerial vehicles (UAV) to inspect the crops periodically and this information is used to establish suitable indication and control operations. That information can be obtained by using suitable camera shots. By using image processing algorithms we can then transform these shots into one large 'orthomosaic' image [10]. By applying algorithms like Normalized Difference Vegetation Index (NDVI) [11] to this image, it is possible to create a reflectance map of crops. These operations can be performed using RGB (Red/Green/Blue), NIR (near-infrared), RE (rededge), multiSPEC 4C (multispectral) [9], thermoMAP (thermal infrared) sensor/cameras. To accomplish all these tasks, it is needed to develop a system capable of controlling and navigating the UAV in an unknown environment using only On-board sensors, without markers or calibration objects. The main sensor to be used is the frontal camera in order to compute an absolute estimate of the drones pose by applying visual tracking methods. This pose estimate can then be used to calculate the control commands required to fly to and hold a desired position in three-dimensional space. This approach enables a UAV to accomplish tasks such as

- Holding a flying position in spite of external disturbances and interference such as wind.
- Challenges include estimating the unknown scale of the visual map, compensating for the large delays present in the system, and dealing with the limited sensor quality available by combining visual pose estimates with additional sensor measurements available. Furthermore the system is required to be robust with respect to temporary loss of visual tracking, missing or corrupted sensor measurements and varying connection quality of the wireless link.

The UAV is attached with the UGV by use of a strong electromagnet. Whenever sample collection or close monitoring is needed UGV is detached from the UAV and instructed to map its environment.

II. METHODS

A. Unmanned Aerial Vehicle

The frame of the UAV influences the stability and robustness during flight. Target weight that is to be lifted is approximated to 1550 gms. We have utilized Beaglebone Black for performing all computations. It is a low cost, open source, single board computer produced by Texas Instruments that can be used to build complex applications that interface highlevel software and low-level electronic circuits. It utilizes Texas Instruments AM335X microprocessor which can perform up to 2 billion instructions per second. In this project Beaglebone Black runs the Linux operating system patched with Texas Instrument-Real-time Operating Kernel for real time processing.

To estimate the position of the UAV, we have used GY80 10DOF IMU (inertial measurement unit). It consists of the following sensors: gyroscope, accelerometer, magnetometer, barometer. Three-axis gyroscope measures angular velocity in all three orthogonal orientations (pitch, roll and yaw). A three axis accelerometer measures how fast the UAV is speeding

978-1-5090-0615-1/16/$31.00 ©2016 IEEE

Fig. 1. Experimental setup

up or slowing down in all three orthogonal directions. Earths gravitation field also affects the accelerometer; this gives an indication of the UAVs orientation with respect to the earth. Both these sensors give a relative reference. Integrating the measurements could give an absolute reference for both the orientation and the position. For an absolute orientation a magnetometer is used. A magnetometer measures the magnetic field of earths magnetic poles, which gives an indication of the absolute orientation of the UAV. An ultrasonic altitude sensor is added in order to obtain the altitude. A barometer and a GPS are also added in order to accurately determine the height. In order to collect multispectral images, a commonly used multispectral sensor, Sequoia is used. It captures both visible and invisible images, providing calibrated data to optimally monitor the health and vigor of your crops. Sequoia captures calibrated wavelength, Green, Red, Red-Edge and Near Infrared to highlight the health of plants. Its applications include visual inspection, elevation modeling, plant counting, soil property & moisture analysis, crop health/stress analysis, water management, erosion analysis, plant physiology analysis, irrigation scheduling, maturity evaluation, yield forecasting.

B. Unmanned Ground Vehicle (UGV)

A rugged UGV robot is used in this system for collection of soil samples to determine nutrient and contaminant content, soil composition and other characteristics such as the acidity or pH level. The UGV robot also utilizes on the Beaglebone Black single board computer. UGV is fitted with LIDAR for 3D mapping [13] and localization and also a high resolution monolithic camera is used to relay real time images to the user.

C. Embedded Linux

The Linux operating system configured and enhanced to work in a wide variety of applications, including handheld devices, network appliances, industrial machines and autonomous robots. For real-time applications, the Linux kernel has been modified by several vendors to provide instant response times. Here the BeagleBone Black runs a Debian installation patched with real time kernel provided by Texas Instruments.

D. Robot Operating System (ROS)

Robot Operating System (ROS) [4] is a collection of software frameworks for robot software development, (see also Robotics middleware) providing operating system-like functionality on a heterogeneous computer cluster. ROS provides standard operating system services such as hardware abstraction, low-level device control, implementation of commonly used functionality, message-passing between processes, and package management. ROS is authorized under an open source, BSD permit. Hector UAV package [8] provided by Johannes Meyer is utilized in this project for simulation in Gazebo [7] and localization testing as shown in fig.2.

Fig. 2. Quadcopter simulation in Gazebo

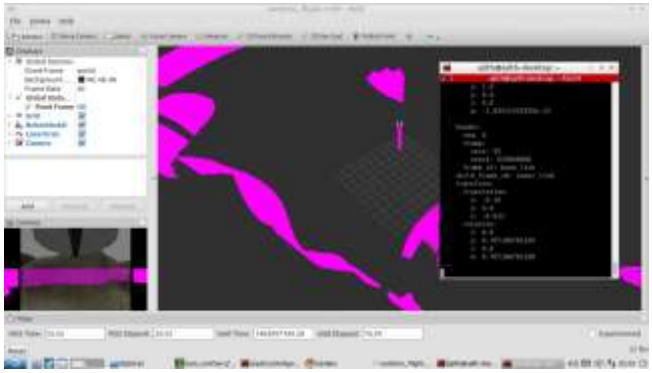

Fig. 3. coordinate frames and transform data

E. Visual SLAM

SLAM stands for the term Simultaneous Localization and Mapping. It is a procedure through which the map of an unknown environment is constructed and updated. SLAM will always use several different types of sensors, and the powers and limits of various sensor types have been a major driver of new algorithms. Statistical independence is the mandatory requirement to cope with metric bias and with noise in measures. Different types of sensors give rise to different SLAM algorithms whose assumptions are which are most appropriate to the sensors. As shown in fig.4 and fig.5, SLAM is performed and visualized in rviz [5] platform and map of an given environment is created.

978-1-5090-0615-1/16/$31.00 ©2016 IEEE

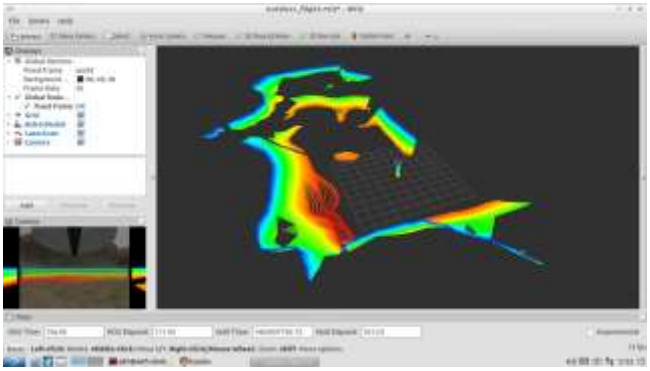

Fig. 4. SLAM visualization in rviz

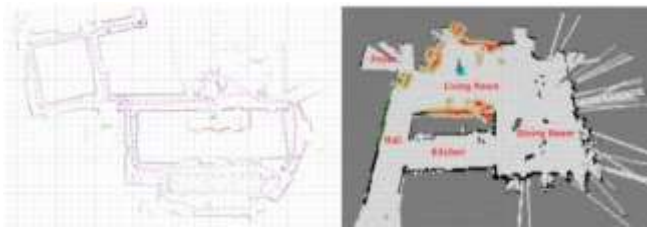

Fig. 5. mapping of given environment

F. Crop Status Mapping

For instance , when two images are of same scene is taken at different positions, there is need to register the second image with the first image. Therefore, a homography needs to be figured out from these images. We adopt Harris corner detector [2] to detect salient feature points in both images. Harris corner detector is a popular image processing tool, and it calculates 2x2 gradient co-variation matrix M over a predefined neighborhood, then it evaluates the determinant and trace of M for every pixel in destination image. Harris corner detector uses autocorrelation function of data. To find the corners in the input image, Harris method uses the average intensity which is directional. Mathematically, Harris corner detector computes the difference in intensity in all direction for a displacement (u, v) .Let $\mathbf{I}(x, y)$ be the gray intensity of pixel (u, v), then with a shift of (u, v), the variation of gray point (x, y) can be represented as

$$E(u,v) = \sum_{x,y} W(x,y)[I(x+u, y+v) - I(x,y)]^2 \qquad (1)$$

In equation (1), $W(x, y)$ represents window function and $\mathbf{I}(x + u, y + v)$ represents the shifted intensity values of $\mathbf{I}(x, y)$.Maximizing the function E(u, v) for corner detection.

$$M = \sum_{x,y} W(x,y) \begin{bmatrix} I_x I_x & I_x I_y \\ I_x I_y & I_y I_y \end{bmatrix} \qquad (2)$$

The eigen values of the matrix given in equation (2) is used to detect the position of point or edge or corner. An equation can be formed which is used to decide whether the region is corner, edge or flat.

$$R = \det(M) - k(\mathrm{trace}(M))^2 \qquad (3)$$

In equation (3), considering, λ_1 and λ_2 as eigen values of M, then $\det(M) = \lambda_1 \lambda_2$, $\mathrm{trace}(M) = \lambda_1 + \lambda_2$

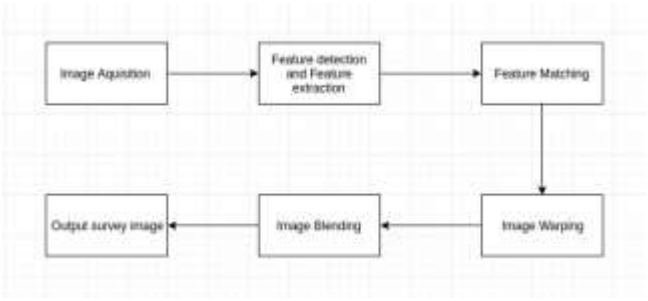

Fig. 6. Image stiching proceedure

Using the detected feature points in the first image, we apply a pyramid Lucas-Kanade method (Lucas and Kanade) [1] to detect the corresponding feature points in the second image [12]. It assumes that the flow is essentially constant in a local neighbor-hood of the pixel under consideration, and solves the basic optical flow equations for all the pixels in that neighbor-hood, by the least squares criterion and approximates the image signal using local Taylor series to derive the spatial and temporal derivatives between image sequences so that the corresponding feature point can be located. Lucas-Kanade method is usually carried out in a coarse-to-fine iterative manner, in such a way that the spatial derivatives are first computed at a coarse scale in a pyramid, one of the images is warped by the computed deformation, and iterative updates are then computed at successively finer scales.

In order to estimate the homography, it is necessary to exclude the errors from the set of correspondence. We use RANSAC [3] algorithm to estimate homography from detected corresponding feature points. RANSAC is very robust for estimating parameters of a mathematical model from a set of observed data which contains outliers, which are data points that do not fit the model. In addition to this, the data points can be subject to noise. RANSAC starts with a random and small set of inliers to estimate the parameters of a model, then tests all of other data points whether the derived model fits the most of data points, if it does then globally optimize the parameters of model by removing outliers and including inliers only. RANSAC can achieve a high degree of accuracy when outliers are present in the data set, and the homography estimated in our scheme are generally satisfied.

G. Normalized Difference Vegetation Index (NDVI)

Vegetation index specifies the greenness, relative density and health of vegetation. To determine the density of green on a patch of land, observation is to be done on distinct colors (wavelengths) of visible and near-infrared sunlight reflected

978-1-5090-0615-1/16/$31.00 ©2016 IEEE

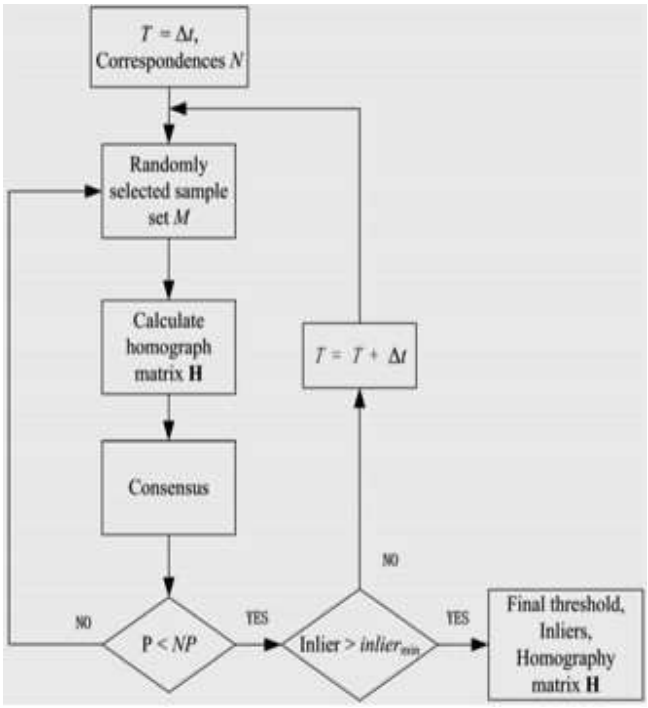

Fig. 7. RANSAC algorithm flowchart

by the plants. When sunlight strikes the plants, certain wavelengths of this spectrum are absorbed and other wavelengths are reflected. The pigment in plant leaves, chlorophyll [6], strongly absorbs visible light (from 0.4 to 0.7 m) for use in photosynthesis. The cell structure of the leaves, on the other hand, strongly reflects near-infrared light (from 0.7 to 1.1 m). The following figure shows the data collected by L.Zhong of California agriculture [14].

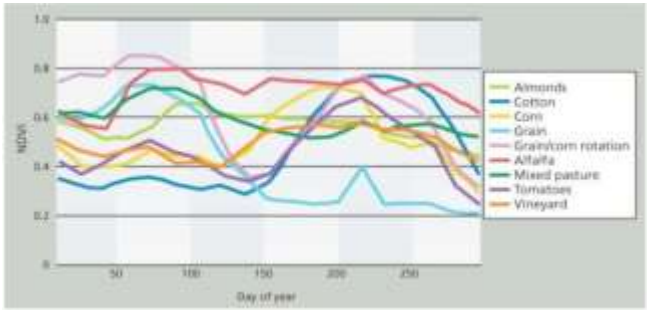

Fig. 8. NDVI data for different plants

This index is a measure of healthy, green vegetation. The combination of its normalized difference formulation and use of the highest absorption and reflectance regions of chlorophyll make it robust over a wide range of conditions. It can, however, saturate in dense vegetation conditions when LAI becomes high.

$$NDVI = \frac{NIR - VIS}{NIR + VIS} \quad (4)$$

where VIS and NIR represents reflectance measurements acquired in the visible (red) and NIR regions. The value of this index ranges from -1 to 1. The common range for green vegetation is 0.2 to 0.8.

Fig. 9. NDVI map calculated with the standard formula

H. Soil Adjusted Vegetation Index (SAVI)

This index is similar to NDVI, but it suppresses the effects of soil pixels. It uses a canopy background adjustment factor,L, which is a function of vegetation density and often requires prior knowledge of vegetation amounts. Huete (1988) suggests an optimal value of L=0.5 to account for first-order soil background variations [5]. This index is best used in areas with relatively sparse vegetation where soil is visible through the canopy.

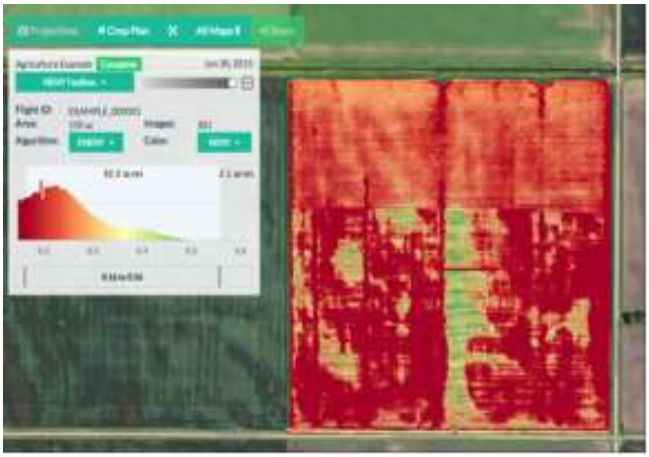

Fig. 10. SAVI map

I. Enhanced Normalized Difference Vegetation Index (ENDVI)

ENDVI includes a comparison of Green light in addition to NIR, Red, and Blue in order to give a more sensitive result. This isolates the indicators of plant health, and can be used to assess the presence and health of a crop.

978-1-5090-0615-1/16/$31.00 ©2016 IEEE

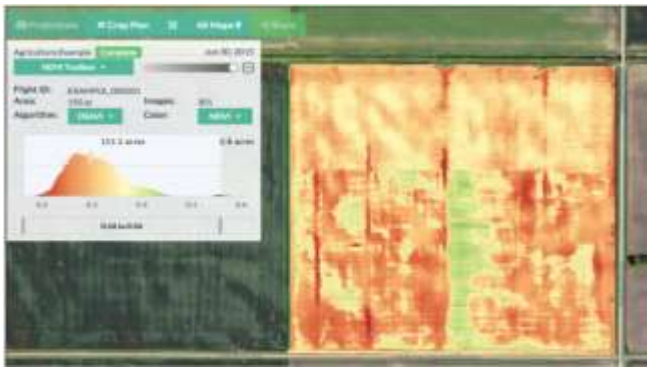

Fig. 11. ENDVI map

J. Optimized Soil Adjusted Vegetation Index (OSAVI)

This index is based on the Soil Adjusted Vegetation Index (SAVI). It uses a standard value of 0.16 for the canopy background adjustment factor. Rondeaux (1996) determined that this value provides greater soil variation than SAVI for low vegetation cover, while demonstrating increased sensitivity to vegetation cover greater than 50%.

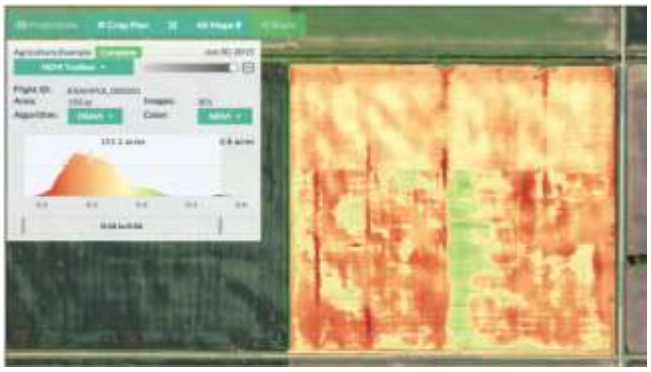

Fig. 12. OSAVI map

This index is best used in areas with relatively sparse vegetation where soil is visible through the canopy.

K. Renormalized Difference Vegetation Index (RDVI)

This index uses the difference between near-infrared and red wavelengths, along with the NDVI, to highlight healthy vegetation. It is insensitive to the effects of soil and sun viewing geometry

III. Conclusion

Quantification of the NVDI and other indices helps to improve the understanding of multispectral data over farmlands areas. The hardware design and the software were described. Data analysis and visualization methodologies were employed to help growers obtain information from acquired data for farm management. Improvements are needed regarding flight length, camera vibration, electromagnet interference, image acquisition. However, further development of sensors could greatly increase the potential of this system.

Fig. 13. RDVI map

References

[1] Jean-Yves Bouguet. Pyramidal implementation of the affine lucas kanade feature tracker description of the algorithm. Intel Corporation, 5(1-10):4, 2001.

[2] Konstantinos G Derpanis. The harris corner detector. York University, 2004.

[3] Konstantinos G Derpanis. Overview of the ransac algorithm. Image Rochester NY, 4:2–3, 2010.

[4] Willow Garage. Robot operating system (ros), 2012.

[5] David Gossow, Adam Leeper, Dave Hershberger, and Matei Ciocarlie. Interactive markers: 3-d user interfaces for ros applications [ros topics]. Robotics & Automation Magazine, IEEE, 18(4):14–15, 2011.

[6] Driss Haboudane, John R Miller, Nicolas Tremblay, Pablo J Zarco-Tejada, and Louise Dextraze. Integrated narrow-band vegetation indices for prediction of crop chlorophyll content for application to precision agriculture. Remote sensing of environment, 81(2):416–426, 2002.

[7] Nathan Koenig and Andrew Howard. Design and use paradigms for gazebo, an open-source multi-robot simulator. In Intelligent Robots and Systems, 2004.(IROS 2004). Proceedings. 2004 IEEE/RSJ International Conference on, volume 3, pages 2149–2154. IEEE, 2004.

[8] J Meyer. Hector quadrotor ros package website, 2014.

[9] Cle Pohl and John L Van Genderen. Review article multisensor image fusion in remote sensing: concepts, methods and applications. International journal of remote sensing, 19(5):823–854, 1998.

[10] S. Schultz, F. Giuffrida, and R. Gray. Mosaic oblique images and methods of making and using same, January 18 2011. US Patent 7,873,238.

[11] John RG Townshend and CO Justice. Analysis of the dynamics of african vegetation using the normalized difference vegetation index. International Journal of Remote Sensing, 7(11):1435–1445, 1986.

[12] Etienne Vincent and Robert Laganiére. Detecting planar homographies in an image pair. In Proceedings of the 2nd International Symposium on Image and Signal Processing and Analysis, pages 182–187, 2001.

[13] Yongjun Zhang, Zuxun Zhang, Jianqing Zhang, and Jun Wu. 3d building modelling with digital map, lidar data and video image sequences. The Photogrammetric Record, 20(111):285–302, 2005.

[14] Liheng Zhong, Peng Gong, and Greg S Biging. Phenology-based crop classification algorithm and its implications on agricultural water use assessments in californias central valley. Photogrammetric Engineering & Remote Sensing, 78(8):799–813, 2012.

978-1-5090-0615-1/16/$31.00 ©2016 IEEE